

# A Time-Resolved NIRS Measurement using High Time-Resolution CMOS Lock-In Pixel Image Sensor

Zhonghui Liu<sup>1</sup>, Min-Woong Seo<sup>2</sup>, Masatsugu Niwayama<sup>1</sup>,  
Keichiro Kagawa<sup>2</sup>, Keita Yasutomi<sup>2</sup>, Shoji Kawahito<sup>2</sup>

<sup>1</sup> Graduate School of Engineering, Shizuoka University 3-5-1 Johoku, Hamamatsu, 432-8011 Japan

<sup>2</sup> Research Institute of Electronics, Shizuoka University 3-5-1 Johoku, Hamamatsu, 432-8011 Japan

E-mail: [liu@idl.rie.shizuoka.ac.jp](mailto:liu@idl.rie.shizuoka.ac.jp)

**Abstract** A CMOS lock-in pixel image sensor with lateral electric field charge modulation (LEFM) is used for time-resolved NIRS (near-infrared spectroscopy) measurement. The developed imager with LEFM achieves a very high time-resolution of tens of picoseconds and a very short intrinsic response time of hundreds of picoseconds. These sensor characteristics help to measure the absorption and scattering coefficients of the biological tissues as well as high time-resolved images.

**Keywords:** NIRS, TRS, fitting method, light propagation formula, scattering coefficient

## 1. Introduction

A near-infrared spectroscopy (NIRS) is a versatile tool for noninvasive evaluation of oxygen saturation in living tissue with a near-infrared light-source. The time-resolved imaging devices make to acquire the absorption coefficient and scattering coefficient simultaneously.

Recently, a CMOS-based high performance time-resolved (TR) image sensor has been developed, which has a high time-resolution, a fast intrinsic response, and a low noise performance. Using the TR CMOS image sensor (CIS) and a theoretical formula of the light propagation, the both coefficients, particularly scattering coefficient, of the specimen are successfully measured.

## 2. Architecture of NIRS measurement system and its implementation

The block diagram of the proposed NIRS measurement system with the TR CIS is shown in Fig.1 and Fig.2. Entire system is composed of FPGA for providing the sensor control signals, a delay controller, a light source (851nm laser diode), an evaluation PCB with the TR CIS, and a specimen.

In the preliminary NIRS experiment, the control signals from the FPGA are transferred into the chip and the trigger signal generated in the chip delivers to the delay controller. The laser light synchronized with the trigger signal penetrates into the specimen, which is the imitated biological tissue. Then the transmitted signal light through the specimen is sampled by the TR CIS. Finally, the reproduced signal distribution is analyzed with the theoretical decay profile.

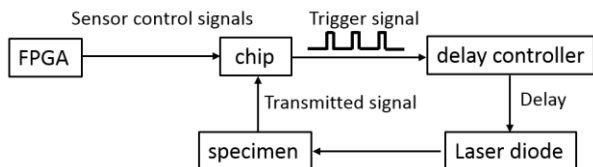


Fig.1. Block diagram of the proposed NIRS system

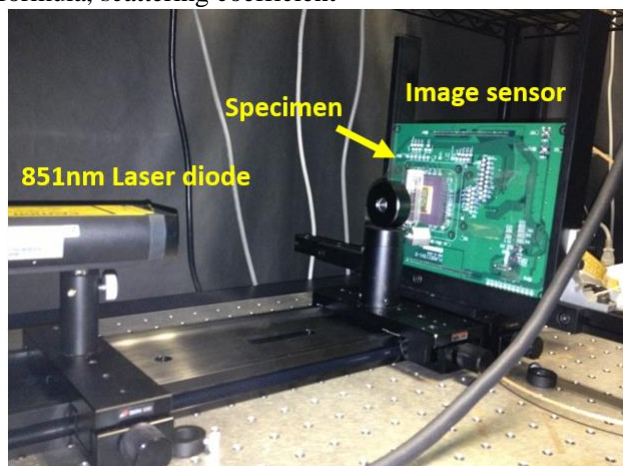


Fig.2. Photograph of the architecture of NIRS measurement

## 3. Experimental results

The experimental results with different specimens are shown in Fig.3. The blue line is for the water, the green line is for the 0.2% intralipid, and the red line is for the 0.4% intralipid. As can be seen from this figure, the measured decay profiles are shifted to the right-hand side by increasing the concentration of intralipid.

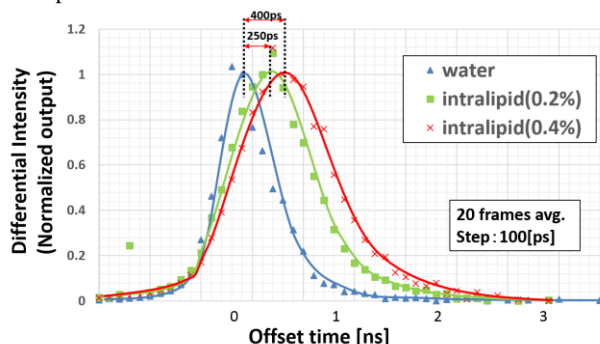


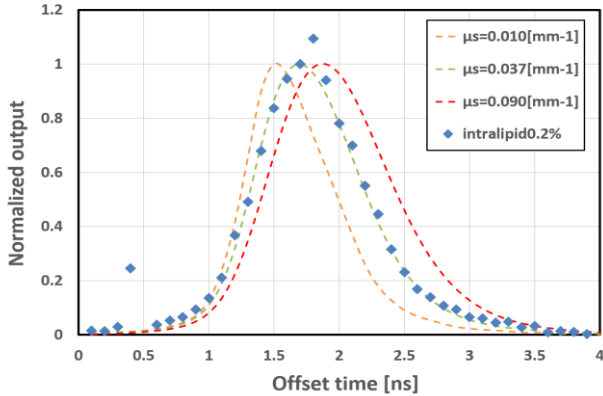
Fig.3. Measurement results with the different specimens

To find out the scattering coefficients from the measured results, the fitting curve method with the theoretical equation is used. The scattering coefficient can be calculated by using the formula of the light propagation expressed as below:

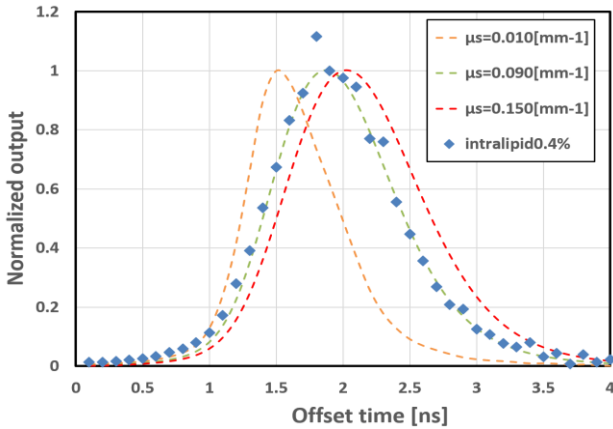
$$T(\rho,t)p = (4\pi Dct)^{-\frac{1}{2}} t^{\frac{3}{2}} \exp(\mu_a ct) \times \left\{ (\rho - z_0) \exp\left[-\frac{(\rho - z_0)^2}{4Dct}\right] - (\rho + z_0) \exp\left[-\frac{(\rho + z_0)^2}{4Dct}\right] + (3\rho - z_0) \exp\left[-\frac{(3\rho - z_0)^2}{4Dct}\right] - (3\rho + z_0) \exp\left[-\frac{(3\rho + z_0)^2}{4Dct}\right] \right\} \quad (1)$$

where,  $T$  is the theoretical transmitted intensity,  $\mu_s$  is the scattering coefficient,  $\mu_a$  is the absorption coefficient,  $D$  and  $z_0$  is the coefficient of  $\mu_s$ ,  $\rho$  is the distance from the point of entry to the detector,  $c$  is the velocity of light. By changing the scattering coefficient, the different decay curves of the theoretical transmitted intensity can be obtained. The scattering coefficient is attained by comparing between the theoretical curves and the measurement results. The comparison results are shown in Fig.4(a) and Fig.4(b).

Fig.4(a) shows the measurement results of 0.2% intralipid and the different theoretical transmitted intensity curves. According to this result, the scattering coefficient of  $0.037\text{mm}^{-1}$  is obtained, when the intralipid concentration is 0.2%. Fig.4(b) shows the measurement results at 0.4% intralipid concentration and the different theoretical transmitted intensity curves. A theoretical transmitted intensity curve with the scattering coefficient of  $0.09\text{mm}^{-1}$  is fitted to the measurement result, which means the scattering coefficient of the measured sample is approximately  $0.09\text{mm}^{-1}$ .



(a)



(b)

Fig.4 (a) Fitted results and measurement results at 0.2% intralipid (b) Fitted results and measurement results at 0.4% intralipid.

Using the high time-resolved CMOS imager, the decay profiles of the imitated biological tissue have been successfully attained. The measured data are compared with the theoretical transmitted intensity curve, and finally, we can confirm the scattering coefficients of samples using the proposed NIRS measurement system.

Additionally, the NIRS system with the TR CIS is very suitable for the pre-diagnosis equipment, e.g., mobile and wearable NIRS device, because the entire system can be integrated and compact.

### Acknowledgments

This work was supported in part by the Grant-in-Aid for Scientific Research (S) under Grant 25220905 through the Ministry of Education, Culture, Sports, Science and Technology (MEXT), in part by the MEXT Grant-in-aid for Scientific Research for Innovative Areas under Grant 25109003, and in part by the MEXT/JST COI-STREAM program.

### References

- [1] S. Kawahito *et al.*, in *Proc. International Image Sensor Workshop (IISW)*, pp. 361-364, Jun. 2013.
- [2] M. W. Seo *et al.*, *Dig. Tech. Papers, ISSCC*, pp. 198-199, Feb. 2015.
- [3] G. Nishimura *et al.*, *Phys. Med. Biol.*, p. 2997, May. 2006.

## 4. Conclusion